17(E)-Picolinylidene androstane derivatives as potential inhibitors of prostate cancer cell growth: Antiproliferative activity and molecular docking studies

ARTICLE *in* BIOORGANIC & MEDICINAL CHEMISTRY · OCTOBER 2013

Impact Factor: 2.79 · DOI: 10.1016/j.bmc.2013.09.063 · Source: PubMed

8 AUTHORS, INCLUDING:

Jovana Ajdukovic
University of Novi Sad
22 PUBLICATIONS **88** CITATIONS
SEE PROFILE

Edward T Petri
University of Novi Sad
30 PUBLICATIONS **383** CITATIONS
SEE PROFILE

Marija N. Sakač
University of Novi Sad
84 PUBLICATIONS **347** CITATIONS
SEE PROFILE

Katarina Penov Gaši
University of Novi Sad
128 PUBLICATIONS **440** CITATIONS
SEE PROFILE

Bioorganic & Medicinal Chemistry 21 (2013) 7257–7266

Contents lists available at ScienceDirect

Bioorganic & Medicinal Chemistry

journal homepage: www.elsevier.com/locate/bmc

17(*E*)-Picolinylidene androstane derivatives as potential inhibitors of prostate cancer cell growth: Antiproliferative activity and molecular docking studies

Jovana J. Ajduković [a,*], Evgenija A. Djurendić [a], Edward T. Petri [c,*], Olivera R. Klisurić [b], Andjelka S. Ćelić [c], Marija N. Sakač [a], Dimitar S. Jakimov [d], Katarina M. Penov Gaši [a]

[a] Department of Chemistry, Biochemistry and Environmental Protection, Faculty of Sciences, University of Novi Sad, Trg Dositeja Obradovića 3, 21000 Novi Sad, Serbia
[b] Department of Physics, Faculty of Sciences, University of Novi Sad, Trg Dositeja Obradovića 4, 21000 Novi Sad, Serbia
[c] Department of Biology and Ecology, Faculty of Sciences, University of Novi Sad, Trg Dositeja Obradovića 4, 21000 Novi Sad, Serbia
[d] Oncology Institute of Vojvodina, Institutski put 4, 21204 Novi Sad, Serbia

ARTICLE INFO

Article history:
Received 11 July 2013
Revised 25 September 2013
Accepted 26 September 2013
Available online 3 October 2013

Keywords:
Androstane
17α-Picolyl and 17(*E*)-picolinylidene derivatives
Synthesis
Antiproliferative activity
Antitumor
Virtual screening
Molecular docking

ABSTRACT

We report a rapid and efficient synthesis of A-ring modified 17α-picolyl and 17(*E*)-picolinylidene androstane derivatives from dehydroepiandrosterone. Compounds were validated spectroscopically and structurally characterized by X-ray crystallography. Virtual screening by molecular docking against clinical targets of steroidal anticancer drugs (ERα, AR, Aromatase and CYP17A1) suggests that 17(*E*)-picolinylidene, but not 17α-picolyl androstanes could specifically interact with CYP17A1 (17α-hydroxylase) with similar geometry and affinity as Abiraterone, a 17-pyridinyl androstane drug clinically used in the treatment of prostate cancer. In addition, several 17(*E*)-picolinylidene androstanes demonstrated selective antiproliferative activity against PC3 prostate cancer cells, which correlates with Abiraterone antiproliferative activity and predicted CYP17A1 binding affinities. Based on these preliminary results, 17(*E*)-picolinylidene androstane derivatives could be a promising starting point for the development of new compounds for the treatment of prostate cancer.

1. Introduction

Nitrogen containing steroidal compounds target a variety of biological processes, and are potential candidates for the treatment of a wide-range of diseases, including breast cancer,[1] prostate cancer,[2–4] leukemia,[5–7] autoimmune diseases,[8] and osteoporosis.[9] Prostate cancer is the second most common cancer among men worldwide, and displays androgen-dependency in approximately 80% of patients;[10] while among women, breast cancer is the second leading cause of cancer deaths today. Breast tumors with a relatively high concentration of ER are termed ER+ and can often be treated successfully with steroid-based anti-hormonal therapy.[11,12] Similarly, several nitrogen containing steroidal compounds have been developed for the treatment of prostate cancer, including Abiraterone, VN/124-1 (galeterone) and VN/85-1 (Fig. 1),[4,13,14] which reduce circulating androgen levels through inhibition of 17α-hydroxylase/17,20-lyase (CYP17), an enzyme required for androgen biosynthesis.[15]

We are interested in the synthesis and characterization of novel steroidal compounds with selective antitumor properties, for use in the development of more effective treatments of breast and prostate cancer. Building on our previous work,[16–18] in the present study we present a facile and efficient synthetic route for the production of new A-modified 17α-picolyl and 17(*E*)-picolinylidene androstane derivatives. Synthesized products were validated by spectroscopy and X-ray crystallography, and screened for antitumor potential by in silico molecular docking and anti-proliferation studies. Molecular docking simulations were performed against known clinical targets of steroidal chemotherapeutic drugs currently used in the treatment of breast and prostate cancer: estrogen receptor α (ERα), androgen receptor (AR), Aromatase (CYP19A1) and 17,20-lyase/17α-hydroxylase (CYP17A1).[4,19] Antiproliferative activity was evaluated against five human cancer cell lines: estrogen receptor negative (ER−) breast adenocarcinoma (MDA-MB-231); estrogen receptor positive (ER+) breast adenocarcinoma (MCF-7); prostate cancer (PC3); human cervical carcinoma

* Corresponding authors. Tel.: +381 21 485 27 33; fax: +381 21 454 065.
E-mail addresses: Jovana.Ajdukovic@dh.uns.ac.rs (J.J. Ajduković), Edward.Petri@dbe.uns.ac.rs (E.T. Petri).

0968-0896/$ - see front matter © 2013 Elsevier Ltd. All rights reserved.
http://dx.doi.org/10.1016/j.bmc.2013.09.063

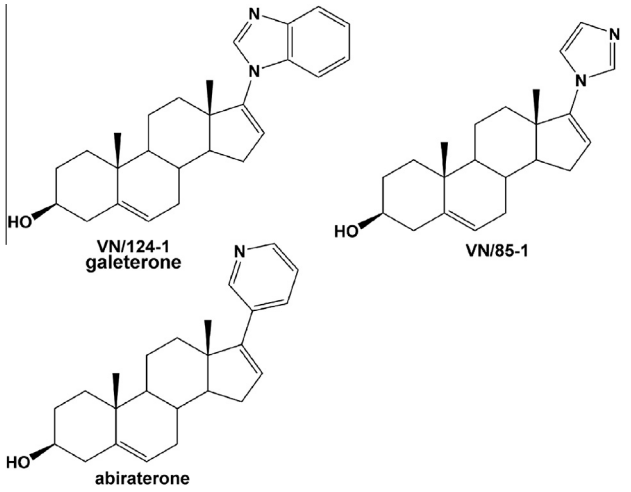

Figure 1. CYP17A1 inhibitors in clinical use (Abiraterone) or under clinical investigation (VN/124-1/galeterone and VN/85-1) for the treatment of prostate cancer.

(HeLa) and colon adenocarcinoma (HT-29). Virtual screening and in vitro anti-proliferation studies suggest that A-modified 17(*E*)-picolinylidene androstane derivatives represent promising candidates for the development of a new series of steroid-based compounds for the treatment of prostate cancer, indicating the need for more detailed future studies.

2. Results and discussion

2.1. Synthesis of novel A-modified 17α-picolyl and 17(*E*)-picol inylidene androstane derivatives

17β-Hydroxy-17α-picolyl-androst-4-en-3-on (**1**) and 17(*E*)-picolinylidene-androst-4-en-3-on (**2**) were used in the synthesis of several new 17α-picolyl and 17(*E*)-picolinylidene derivatives.[17] Initially, compounds **1** and **2** were reacted with hydrazine hydrate, under microwave-assisted heating (195 °C, 170 W for 4 or 2 min) to obtain 17β-hydroxy-17α-picolyl-androst-4-en-3-hydrazone (**3**) and 17(*E*)-picolinylidene-androst-4-en-3-hydrazone (**4**) (Scheme 1). Reaction completion was monitored by NMR: the broad signals at 6.67 and 6.45 ppm in the ^{1}H NMR spectra of compound **3** and **4** (S1), respectively, indicate the presence of two protons from the hydrazone functions, while signals for C-3 atoms were observed at 158.31 or 158.73 ppm in ^{13}C NMR spectra for compounds **3** or **4**. The resulting hydrazone derivatives **3** and **4** were then subjected to a modified Wolff–Kishner reduction under microwave irradiation (195 °C, 170 W, 10 min for **3** or 40 min for **4**). Although we expected to obtain compounds with a Δ^4 system, **7a** (17α-picolyl) or **7b** (17-picolinylidene), Wolff–Kishner reduction led to decomposition of hydrazone **3**; while only a mixture of 5α- and 5β-androst-3-en 17(*E*)-picolinylidene derivatives **5**

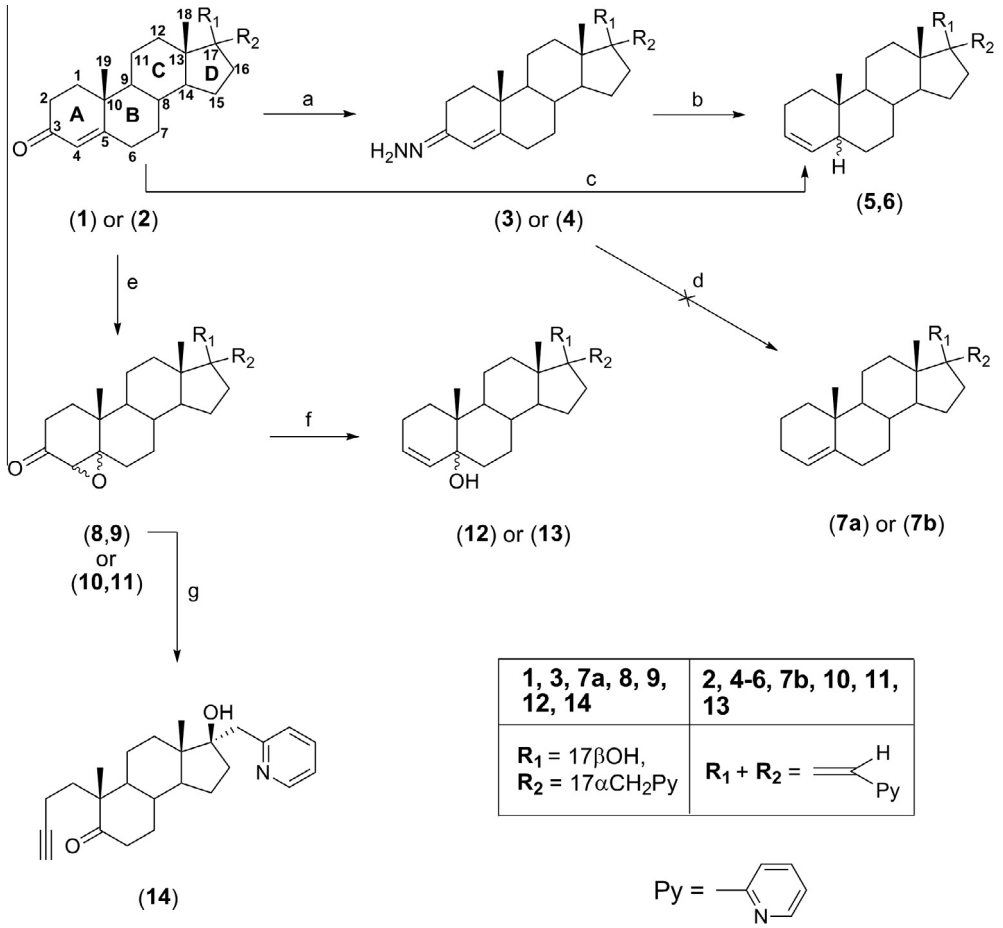

Scheme 1. Reagents and reaction conditions: (a) $NH_2NH_2{\cdot}H_2O$, $OH(CH_2)_2OH$, 195 °C (170 W), 4 min (for **3**) or 195 °C (170 W), 2 min (for **4**); (b) $NH_2NH_2{\cdot}H_2O$, $OH(CH_2)_2OH$, KOH, 195 °C (170 W), 40 min; (c) AcOH, Zn powder, reflux, 2 h; (d) $NH_2NH_2{\cdot}H_2O$, $OH(CH_2)_2OH$, KOH, 195 °C (170 W), 10 min; (e) 30% H_2O_2, 4 M NaOH, MeOH, 0 °C, 1 h → 10 °C, 24 h; (f) $NH_2NH_2{\cdot}H_2O$, 120 °C, 30 min; (g) *p*-$TsNHNH_2$, 50% ethanol, rt, 1 h → 55 °C, 1 h.

and **6** (which could not be separated) was obtained from hydrazone **4**. Similar reactivity was observed for certain 17α-picolyl derivatives under alkaline conditions in our previous work.[20] During Wolff–Kishner reduction of compound **4**, the Δ^4-3-hydrazone undergoes a double-bond migration to give Δ^3-5α and Δ^3-5β olefins as major products.[21] The same mixture of products, **5** and **6**, was also obtained using an alternative reaction protocol, by Clemmensen reduction of 4-en-3-on derivative **2**. The introduction of a Δ^3 double bond in compounds **5** and **6** was confirmed by the presence of an ^{1}H NMR multiplet at 5.31 ppm for H-3 atoms, and doublets at 5.56 and 5.66 ppm, corresponding to H-4 protons from 5α and 5β isomers, respectively (S1). Similarly, ^{13}C NMR spectra displayed characteristic signals for vinyl C-3 and C-4 atoms, at 125.48 and 131.25 ppm for the 5α isomer, or at 127.10 and 132.13 ppm for the 5β isomer.

Compound **1** (or **2**) was further transformed into a mixture of 4α,5α- and 4β,5β-epoxides **8** and **9** (or **10** and **11**) with 30% hydrogen peroxide under alkaline conditions, and recrystallization (from dichloromethane/hexane) afforded pure 4β,5β-isomers **9** and **11**, respectively.[16] Using a Wharton reaction, the mixture of 17α-picolyl epoxides **8** and **9**, or 17(*E*)-picolinylidene epoxides **10** and **11**, was transformed into the new 17α-picolyl-androst-3-en-5α,17β-diol (**12**) or 17-picolinylidene-androst-3-en-5α-ol (**13**). In corresponding ^{1}H NMR spectra, indicative multiplets were observed for H-3 atoms at 5.84 and 5.81 ppm, and doublets were visible for H-4 atoms at 5.54 and 5.51 ppm for compounds **12** and **13**, respectively (S1). Signals which are exchangeable in the presence of D_2O were recorded at 5.61 ppm (for **12**) or 5.30 ppm (for **13**), corresponding to 5-hydroxy group protons. ^{13}C NMR spectral signals were assigned for double bond carbons at 130.84 (C-3) and 133.60 (C-4) ppm for compound **12**, or at 130.84 (C-3) and 133.43 (C-4) ppm for compound **13**. C-5 carbon signals for compounds **12** and **13** were visible at 71.93 and 71.87 ppm (S1).

Epoxides **8** and **9** were also transformed by Eschenmoser fragmentation into the new 17β-hydroxy-17α-picolyl-4,5-secoandrost-3-yn-5-one (**14**). IR spectra bands at 2116 and 1700 cm^{-1} indicate the presence of an acetylenic and C_5-keto function (S1). Also, analysis of ^{13}C NMR spectra of compound **14** confirmed the expected A-seco structure with signals at 68.07, 83.16 and 214.46 ppm, for C-3, C-4 and C-5 atoms, respectively. The complete structure and relative stereochemistry of **14** was established by X-ray diffraction analysis (Figs. 2 and S2), and crystallographic data was deposited at the Cambridge crystallographic data centre (CCDC 948404).

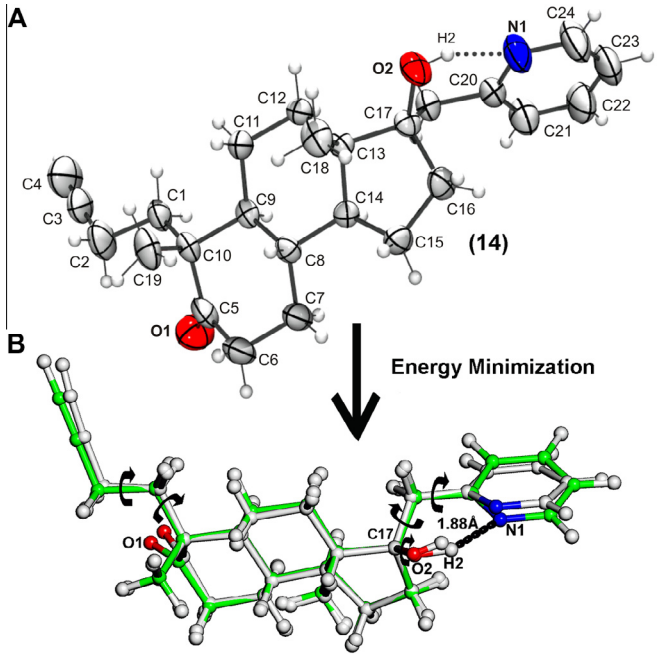

Figure 2. (A) X-ray crystal structure of compound **14**. (B) MOPAC-PM6 energy minimized structure of compound **14**. The positions of hydrogen atoms in the X-ray crystal structure of compound **14** (white cpk) were optimized using MOPAC PM6–DH2 and the resulting structure was subjected to conjugate gradient energy minimization using an MMFF94 force field (green cpk). The H2...N1 hydrogen bond distance changes from 2.03 to 1.88 Å. Rotatable bonds are labeled with arrows.

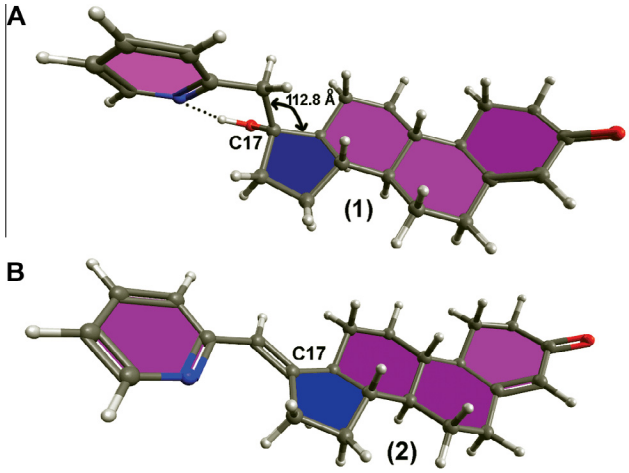

Figure 3. Energy minimized X-ray crystal structures of (A) compound **1**, which contains a 17α-picolyl group, and (B) compound **2**, which contains a 17-picolinylidene group. Structural co-ordinates resulting from energy minimization were used as templates to create three-dimensional structural models of compounds **1**–**14** for molecular docking studies.

Because we observed an intra-molecular hydrogen bond involving the 17α-picolyl nitrogen atom and the C17β-hydroxyl group in the X-ray crystal structure of compound **14**, the molecular geometry of **14** was further analyzed by energy minimization. Positions of hydrogen atoms in the structure were refined using MOPAC PM6-DH2[22] followed by conjugate gradient energy minimization using an MMFF94 force field.[23] As can be seen in Figure 2B, the H2...N1 hydrogen bond distance improves from 2.03 to 1.88 Å, and the hydrogen bond angle becomes more planar, suggesting that this bond could be energetically favorable. Similar intramolecular hydrogen bonds were observed in the energy minimized X-ray crystal structure of compound **1** (Fig. 3A) and in all energy minimized 17α-picolyl androstane structural models (S3b).

2.2. In vitro antiproliferative activities and structure–activity relationships of A-ring modified 17-picolyl and 17-picolinylidene androstane derivatives

Previously, we reported the cytotoxic activities of several compounds (**1**, **2**, **9** and **11**) with 17α-picolyl or 17(*E*)-picolinylidene substituent groups.[16,17] In the present study, we combine these results with those obtained for newly synthesized compounds **3**–**6** and **12**–**14** to develop preliminary structure–activity relationships for use in the future design of more effective compounds.

The in vitro antiproliferative activities of A-ring modified 17α-picolyl and 17(*E*)-picolinylidene androstane derivatives **1**–**4**, and **9**, **11**–**14** were evaluated against several common types of cancer cell lines (human breast adenocarcinoma ER+ (MCF-7), human breast adenocarcinoma ER− (MDA-MB-231), prostate cancer (PC3), human cervical carcinoma (HeLa) and colon cancer (HT-29) using the standard MTT assay, after exposure of cells to test compounds. Normal fetal lung fibroblast (MRC-5) cells were used as a cytotoxicity control. Results were compared with the nonselective

Table 1
Antiproliferative activity of compounds **1**–**4**, **9** and **11**–**14** against a panel of human tumor cell lines

Compd	MCF-7	MDA-MB-231	PC-3	HeLa	HT-29	MRC-5
Antiproliferative activity (IC_{50} μM)						
1[16]	>100	>100	>100	—	—	>100
2[16]	>100	>100	12.9	—	—	>100
3	6.3	32.5	>100	>100	>100	>100
4	13.6	17.1	5.9	>100	51.7	>100
9[15]	>100	10.4	65.5	—	—	>100
11[15]	50.7	88.3	14.3	—	—	>100
12	>100	>100	>100	>100	>100	>100
13	>100	>100	>100	49.4	57.2	>100
14	>100	>100	>100	>100	6.5	>100
Doxorubicin	0.75	0.12	95.61	1.17	0.32	0.12
Formestane	>100	55.5	48.36	5.55	>100	>100

cytotoxic drug doxorubicin (DOX), and the steroidal aromatase inhibitor formestane, which was used as a control for general steroidal toxicity. Note that doxorubicin was extremely toxic to normal noncancerous MRC-5 cells, consistent with its nonspecific cellular cytotoxicity. In addition, doxorubicin controls showed low cytotoxicity against PC3 cells (IC_{50} 95.6 μM), which was expected according to David-Beabes et al.[24]

Based on calculated IC_{50} values, several of the synthesized compounds demonstrated significant antiproliferative activity against human breast or prostate cancer cell lines, but were devoid of cytotoxicity toward normal noncancerous control cells (Table 1). Furthermore, compound **14** was found to selectively inhibit the growth of only colon cancer cells (HT-29), among the cell lines tested, and was completely nontoxic to all other cells, suggesting this compound could be an interesting starting point for further investigation. Improving the selectivity of anti-tumor compounds for specific cancer cells, while reducing cytotoxicity toward normal healthy cells, is an important goal of medicinal chemistry.

With respect to breast cancer cells, both compounds **3** (17α-picolyl) and **4** (17-picolinylidene), with a 3-hydrazone substituent, exhibited strong antiproliferative activity (IC_{50} = 6.3 and 13.6 μM) against MCF-7 cells in comparison with corresponding compounds **1** (17α-picolyl) and **2** (17-picolinylidene), with a 3-keto function, which were completely inactive. In addition, compound **3** (IC_{50} = 32.5 μM) and **4** (IC_{50} = 17.1 μM) also showed moderate cytotoxicity against MDA-MB-231 (ER−) breast cancer cells, while **1** and **2** were inactive, suggesting the importance of the 3-hydrazone function for breast cancer cell cytotoxicity. Importantly, 17α-picolyl androstane derivative **3** displayed significant selective inhibition of MCF-7 (ER+) breast cancer cells, suggesting anti-hormonal properties, while compound **9** selectively inhibited only ER− MDA-MB-231 breast cancer cells.

Interestingly, with respect to prostate cancer cells, 17-picolinylidene androstane derivatives **2**, **4** and **11** displayed strong antiproliferative activity against PC3 prostate cancer cells; while the corresponding 17α-picolyl androstane derivatives **1**, **3** and **9** were nontoxic to these cells. In our previous work, 17α-picolyl androstane derivatives 17α-picolyl-androst-5-en-3β,17β-diol and 17β-hydroxy-17α-picolyl-androst-4-ene-3,6-dione also showed marked cytotoxicity against PC3 cells (6.3 and 4.3 μM, respectively: note that these results were obtained using a different measure of cytotoxicity, the sulforhodamine B/SRB assay).[18] Further comparison of the antiproliferative activities of 3-keto derivative **2** (IC_{50} = 12.9 μM) and 3-hydrazone derivative **4** (IC_{50} = 5.9 μM) against PC-3 cells revealed that compound **4** was approximately two-fold more potent than compound **2**, possibly supporting the importance of the 3-hydrazone group over the 3-keto function. However, among the cell lines tested, compound **2** selectively inhibited the growth of only PC3 prostate cancer cells, while compound **4** also inhibited the growth of ER+ (MCF-7) and ER− (MDA-MB-231) breast cancer cell lines, indicating the activity of compound **2** could be more prostate cancer specific. The development of compounds with improved selectivity for particular types of tumor cells could reduce the side effects of chemotherapy, leading to more effective cancer treatments.

Importantly, because none of the tested 17α-picolyl androstane derivates were found to inhibit the growth of PC3 cells, our results strongly suggest that the 17(*E*)-picolinylidene functional group could be responsible for the observed antiproliferative activity against prostate cancer cells.

2.3. In silico virtual screening of 17-picolyl and 17-picolinylidene androstane derivatives by molecular docking

To begin to identify potential protein targets for A-ring modified 17α-picolyl and 17(*E*)-picolinylidene androstane compounds, and to serve as a guide for future investigations, preliminary virtual screening was conducted using molecular docking. To increase the reliability of the molecular models used for ligand compounds **1**–**14**, structural co-ordinates derived from energy minimization of the X-ray crystal structures of compounds **1**, **2** and **14** were used as templates to create three-dimensional structural models for molecular docking studies (Figs. 3 and S3a and S3b).

Molecular docking simulations were performed against known targets of steroidal chemotherapeutic drugs currently used in the treatment of breast and prostate cancer. Protein targets were chosen for virtual screening according to the following criteria: (1) a high-resolution X-ray crystal structure is available in complex with a steroidal ligand or drug; and (2) the protein is a target of clinically-approved steroid-based anti-cancer drugs in the treatment of hormone-dependent breast or prostate cancer. In order to reduce the chance of model bias, docking simulations were conducted using randomized starting ligand co-ordinates and the entire protein as a search space, without pre-defining the ligand binding site. Because of the increased computational power required by this search space, high-throughput molecular docking simulations were facilitated through use of a remote supercomputer cluster at the National Biomedical Computational Resource

Table 2
Predicted binding energies of compounds **1**–**14** calculated from molecular docking against known protein targets of steroidal anti-cancer drugs: CYP17A1 (17a-hydroxylase/17,20-lyase); CYP19A1 (Aromatase); estrogen receptor (ERα) and androgen receptor (AR). Binding energies of ligands present in the X-ray crystal structures were calculated following re-docking

Compound	CYP17A1	CYP19A1	ERα	AR
Autodock binding energy (kcal/mol)				
1	—	—	—	−11.19
2	−12.19	—	—	—
3	—	—	—	—
4	−11.88	—	−7.98	—
5	−10.60	—	—	—
6	−11.12	—	—	—
7a[a]	—	—	—	—
7b[a]	−10.77	—	—	—
8	—	—	—	—
9	—	—	−10.88	—
10	−10.17	—	—	—
11	−10.98	—	—	—
12	—	−7.85	—	—
13	−11.62	—	—	—
14	—	−6.26	—	—
Abiraterone	−11.84			
Androstenedione		−12.56		
Estradiol			−10.22	
DHT				−11.04

[a] Note: synthesis of compounds **7a**,**b** was not successful.

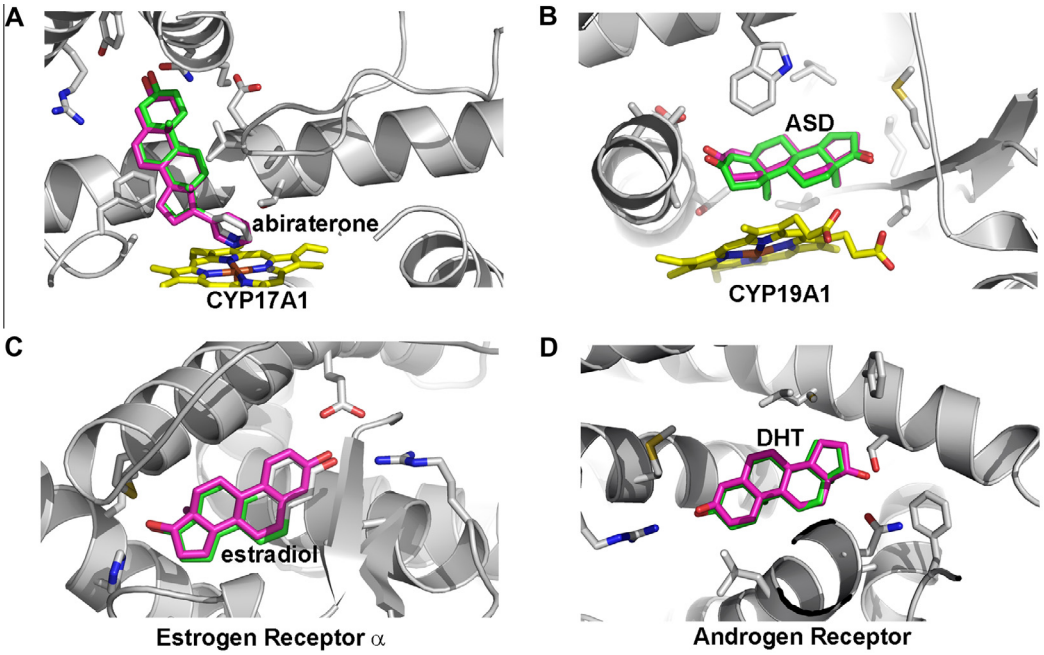

Figure 4. Autodock re-docking of ligands present in the X-ray crystal structures of protein targets used in molecular docking simulations: (A) Abiraterone in complex with CYP17A1 (17α-hydroxylase/17,20-lyase); (B) androstenedione (ASD) in complex with CYP19A1 (Aromatase); (C) estradiol in complex with estrogen receptor (ERα) and (D) dihydrotestosterone (DHT) in complex with androgen receptor (AR). The RMSD between re-docked ligands and the corresponding X-ray crystal structure co-ordinates was ⩽0.6 Å for all cases.

(http://nbcr-222.ucsd.edu/opal2).[25] Remote molecular docking experiments were further facilitated using the virtual screening tool, PyRx.[26] Three-dimensional structural co-ordinates for protein receptors were obtained from the protein data bank (http://www.rcsb.org).

Using the above criteria, molecular docking was performed using the program Autodock[27] for each synthesized compound against X-ray crystal structures of human CYP17A1 (17a-hydroxylase/C17,20-lyase, PDB ID: 3RUK),[14] CYP19A1 (aromatase, PDB ID: 3EQM),[28] estrogen receptor (ERα, PDB ID: 1A52)[29] and androgen receptor (AR, PDB ID: 2AMA)[30] (Table 2 and S4). Both 17α-hydroxylase and aromatase are steroid binding cytochrome 450 enzymes involved in steroidogenesis,[14,28] while ERα and AR serve as steroid receptors for estrogens and androgens, respectively.[29,30] Control autodock docking experiments were conducted using ligands present in the X-ray crystal structures of the receptors. All control re-docking simulations were able to reproduce the ligand–protein interaction geometries present in the respective crystal structures with an RMSD ⩽ 0.6 Å (Fig. 4). In fact, docked ligand structures fit well within experimental $2F_o–F_c$ electron density maps associated with the receptor X-ray crystal structures (S5). Based on these control docking simulations, predicted binding energies ⩽−10.00 kcal/mol were considered to be significant.

As can be seen in Table 2, very strong binding energies (⩽−10.00 kcal/mol) were predicted for eight of the 15 compounds for the active site of CYP17A1 (compounds **2**, **4**–**6**, **7b***, **10**, **11** and **13**; *not synthesized) while no significant binding was observed for any of the compounds for the active site of aromatase. Because both CYP17A1 and CYP19A1 are cytochrome P450 enzymes with the same overall three-dimensional fold (see S6 for a structure-based alignment of CYP17A1 and CYP19A1), our results suggest that these interactions are specific to CYP17/17α-hydroxylase. Strikingly, all of these compounds contain 17(*E*)-picolinylidene functions, and none of the corresponding 17α-picolyl androstane derivatives were predicted to bind CYP17A1, strongly suggesting that the planar, sp2 hybridization geometry imposed on C17 by the 17-picolinylidene function is essential for CYP17A1 binding. Chemical database searches revealed similarities between several of the synthesized compounds and the steroidal drug Abiraterone, which contains a 17-pyridinyl group.[14] Similarities were also found with experimental anti-prostate cancer drugs VN/124-1 (galeterone) and VN/85-1.[4,13] Abiraterone, VN/124-1 (galeterone) and VN/85-1[4,13,14] disrupt androgen biosynthesis via inhibition of 17α-hydroxylase/17,20-lyase (CYP17A1), a key steroidogenic cytochrome P450 enzyme necessary for androgen production.[15] Interestingly, the C17 atom in Abiraterone, VN/124-1 and VN/85-1 is also planar, but due to the presence of a double bond between C16 and C17. Moreover, X-ray crystal structures of Abiraterone

Table 3
Ranking of compounds **1**–**14** by potential antitumor activity against prostate cancer based on predicted 17α-hydroxylase affinity, Heme Fe co-ordination potential, solubility (*c*Log*P*) and experimental cytotoxicity against PC3 cells (IC_{50} μM)

Compd	CYP17A1 docking energy (kcal/mol)	Pyridine N–Heme Fe distance (Å)	Prostate cancer antiproliferative activity (PC3 cells, IC_{50} μM)	*c*Log*P*
4	−11.88	2.87	5.9	4.98
2	−12.19	2.66	12.9	4.93
11	−10.98	3.95	14.3	4.41
10	−11.03	2.97	—	4.41
13	−11.62	2.91	>100	5.30
7b	−10.77	3.54	—	6.33
6	−11.12	2.84	—	6.52
5	−10.60	3.73	—	6.52
8,9	No binding	—	65.5[b]	3.41
1	No binding	—	>100	4.06
3	No binding	—	>100	4.08
12	No binding	—	>100	4.26
14	No binding	—	>100	4.19
Abiraterone	−11.84	2.04	9.32[a]	4.44

[a] Ref. 15.
[b] PC3 IC_{50} values shown for compound **9**.

and VN/124-1 have been solved in complex with CYP17A1, revealing direct co-ordination between the 17-pyridinyl nitrogen and the heme iron of CYP17.[14] In addition to CYP17 inhibition, Abiraterone, VN/124-1 and VN/85-1 have also been shown to inhibit the growth of androgen insensitive prostate cancer cell lines, such as PC-3 cells: in the case of VN/124-1, this has been shown to occur via induction of the endoplasmic reticulum (ER) stress response, resulting in calcium release from the ER and G1 phase cell cycle arrest.[15]

Because structurally similar CYP17A1 inhibitors (including Abiraterone) have been approved for the treatment of prostate cancer,[4] and have been associated with strong antiproliferative effects against PC3 prostate cancer cell lines,[4,13,15] we investigated the correlation between our predicted molecular docking results and PC3 anti-proliferative activity. Furthermore, since circulating concentrations of VN/124-1 >20 μM have been reported to be well-tolerated in LAPC4 mouse models of prostate cancer,[31] IC_{50} values in the low micromolar range for PC3 antiproliferative activity could be physiologically relevant. In order to suggest potential leads for the development of novel steroidal treatments for prostate cancer, compounds were ranked according to their similarities with the known activities of Abiraterone: (1) predicted 17α-hydroxylase affinity;[4] (2) binding orientation to 17α-hydroxylase;[14] (3) Heme-Fe co-ordination potential;[14] (4) solubility as *c*Log*P*;[32] and (5) experimental antiproliferative activity against PC3 cells (IC_{50} μM).[15] Interestingly, three compounds (**2**, **4** and **11**) with strong molecular docking binding energies for CYP17A1 also displayed significant antiproliferative activities against PC3 prostate cancer cells, comparable to those reported for Abiraterone.[15]

Comparison with control docking studies using Abiraterone indicate that **2**, **4**, and **11** could bind CYP17A1 with similar affinity and orientation (Table 3). Furthermore, superposition of the binding geometries of the top two compounds (**2** and **4**) with the X-ray crystal structure of Abiraterone in complex with CYP17A1 reveals that the nitrogen atom at position 2 in the 17(*E*)-picolinylidene function is in an ideal position to co-ordinate with the Heme-Fe atom, in a similar manner to the pyridinyl nitrogen at position 3 in Abiraterone (Fig. 5).[14] Importantly, both ligand geometries allow for co-ordination between the nitrogen atom and the Heme Fe atom, with an N–Fe distance of 2.66 and 2.87 Å, for compounds **2** and **4**, respectively, compared to the N–Fe distance of 2.04 Å measured from the Abiraterone/CYP17A1 crystal structure. Furthermore, both nitrogen atoms are 3.7 Å from the C17 carbon atom (Fig. 5), in agreement with the C17…N distance measured in the CYP17/Abiraterone crystal structure.[14] Finally, both compounds **2** and **4** form hydrogen bonds between their C3 hydrophilic group and N202 in the active site of CYP17, similar to that found in the

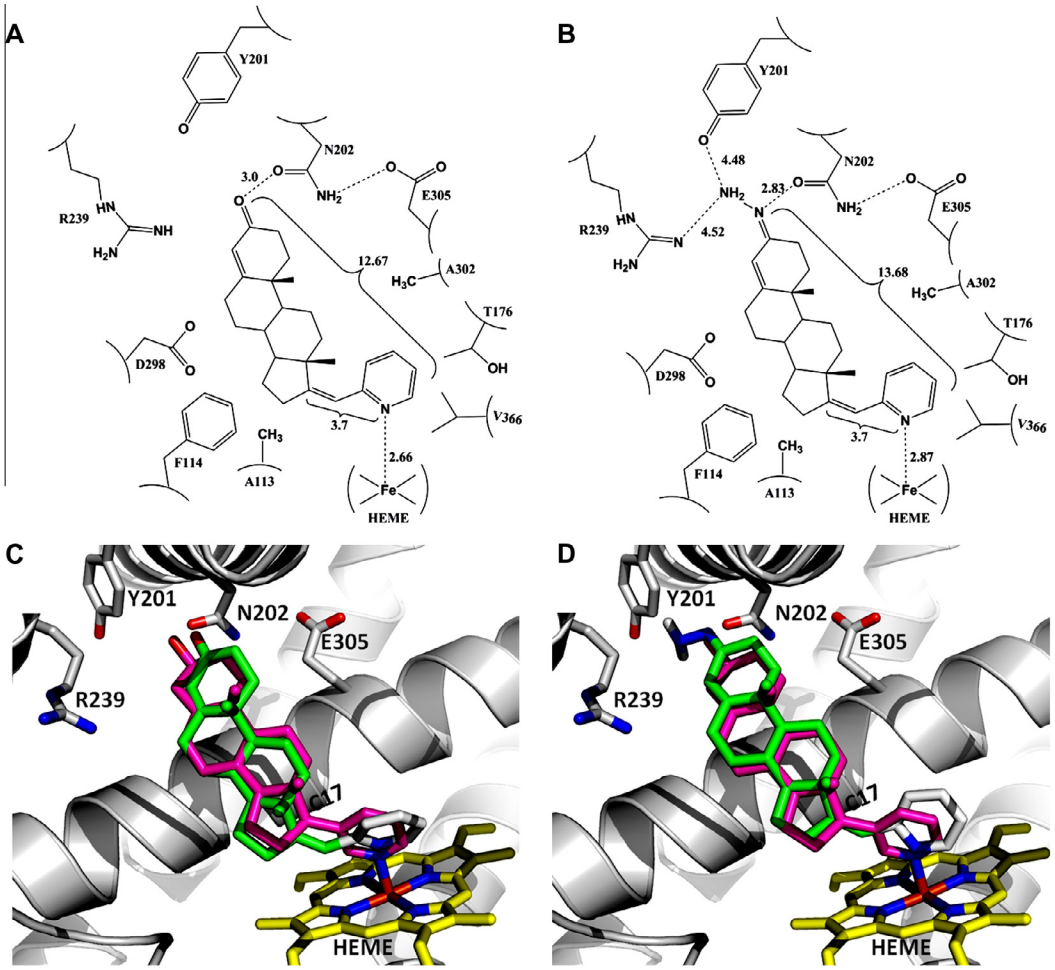

Figure 5. Analysis of predicted CYP17A1 binding orientations for compounds **2** and **4**. Autodock molecular docking results for top ranking compounds **2** (panels A and C) and **4** (panels B and D) are shown. Panels A and B show 2D schematics of residues involved in ligand binding based on the three-dimensional molecular docking results shown in panels C and D. All contact distances and hydrogen bonding distances are shown in angstroms as dotted lines. Compounds **2** and **4** (shown in green) are predicted by Autodock molecular docking simulations to bind to CYP17A1 in a similar orientation and with similar affinity as the clinically approved CYP17A1 inhibitor Abiraterone (magenta).

CYP17/Abiraterone crystal structure. The remaining 17(*E*)-picolinylidene containing compounds (**5**–**7** and **13**) have unusually high calculated partition coefficient values (*c*Log*P*—calculated using ALOGPS 2.1 http://vcclab.org/lab/alogps/),[32] consistent with high hydrophobicity which possibly limits their effective cytotoxicity (Table 3). More importantly, no PC3 antiproliferative activity (IC_{50} >100 μM) was detected for 17α-picolyl containing androstane compounds predicted not to bind to CYP17A1 in molecular docking studies.

In order to further explore the structural basis for the predicted preference of CYP17A1 for 17(*E*)-picolinylidene over 17α-picolyl androstane derivatives, we conducted manual docking simulations. Manual positioning of 17α-picolyl containing androstane derivatives results in severe steric clashes and van der Waals overlap between the 17α-picolyl function and the heme moiety in CYP17A1, which would prevent ligand binding (Fig. 6A). These structural clashes are attributed solely to the tetrahedral sp^3 geometry of the C17 atom in the 17α-picolyl containing androstane derivatives (Fig. 6B) versus the planar sp^2 geometry found at C17 in the 17-picolinylidene androstane derivatives (see Fig. 3B).

Because PC3 cells do not express androgen receptor, the PC3 antiproliferative activity displayed by compounds **2**, **4** and **11** (this study), and by Abiraterone, VN/85-1 and VN/124-1,[15] may not be due solely to CYP17A1 inhibition activity. While previous reports suggest a possible mechanism for PC3 growth inhibition through disruption of calcium homeostasis and induction of ER stress,[15] possible protein target(s) of these steroidal compounds in PC3 cells remain to be identified. However, a clear correlation does exist between PC3 antiproliferative activity, CYP17 inhibitory activity and anti-prostate cancer activity for Abiraterone, VN/124-1 and VN/85-1.[14,15] Thus, taken together, our preliminary molecular docking and

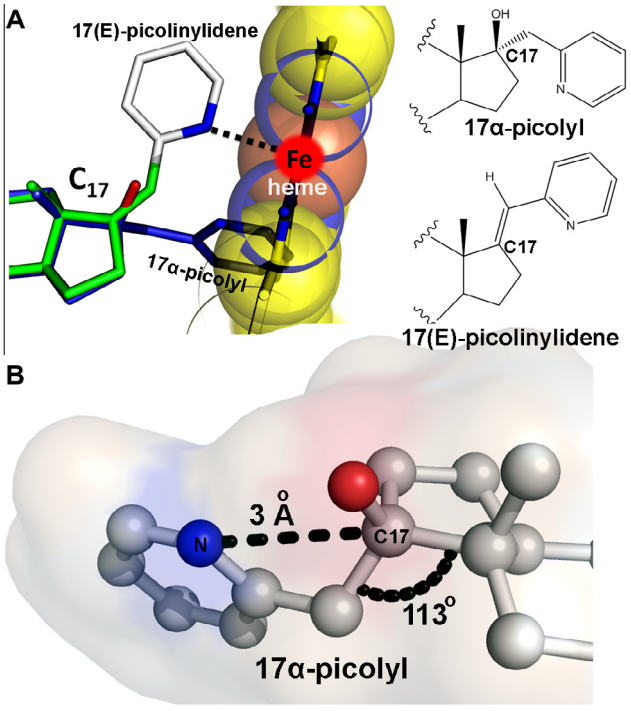

Figure 6. (A) Manual docking of compound **1** onto the crystal structure of CYP17A1 in complex with Abiraterone. The 17α-picolyl group of compound **1** clashes severely with the heme group of CYP17A1, due to the sp^3 tetrahedral geometry of its attachment to C17, explaining the lack of binding observed in Autodock molecular docking simulations. In contrast, the nitrogen at position 2 in the 17-picolinylidene group of compound **4** is in an ideal position for heme co-ordination, due in part to the planar sp^2 geometry of C17. (B) The 17α-picolyl group in the crystal structure of **14**, illustrating the tetrahedral sp^3 geometry of the 17α-picolyl attachment.

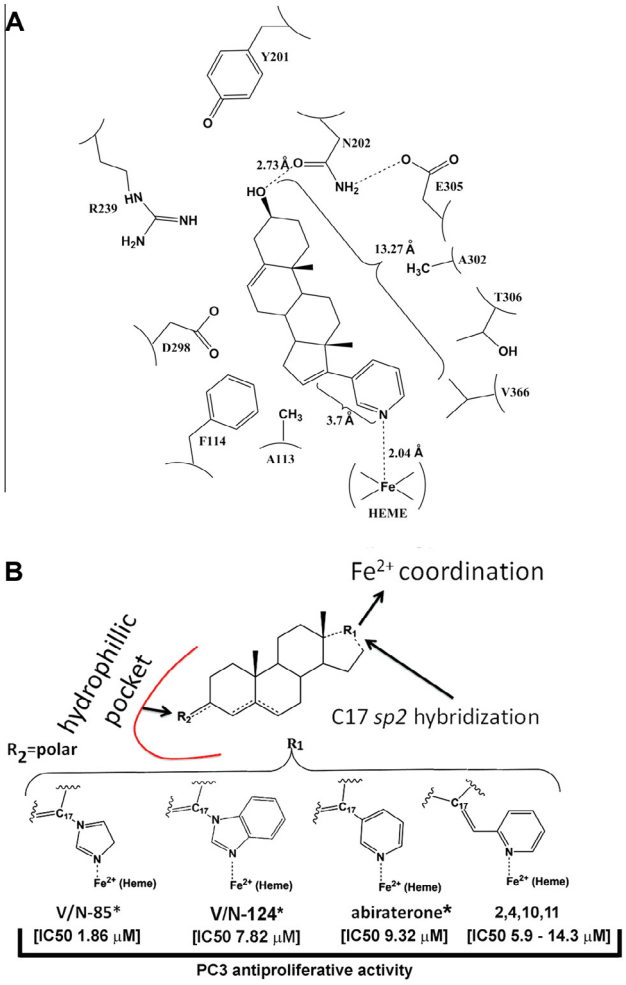

Figure 7. (A) Two-dimensional schematic of Abiraterone binding to CYP17A1. (B) Proposed guide for the synthesis of potential steroidal CYP17A1 inhibitors with antiproliferative activity against PC3 prostate cancer cells.

cytotoxicity studies suggest that 17-picolinylidene androstane derivatives **2** and **4** could be promising potential lead compounds for the development of new steroidal drugs for the treatment of prostate cancer. In particular, compounds **2** and **4** could be used as templates to design a new series of 17(*E*)-picolinylidene androstane derivatives for detailed 17α-hydroxylase/17,20-lyase enzymatic inhibition and kinetics studies, to confirm and extend the preliminary results presented here. Promising lead compounds could also be subjected to extensive anti-tumor trials in vivo.

3. Conclusions

In conclusion, we have successfully synthesized novel A-modified 17α-picolyl and 17(*E*)-picolinylidene androstane derivatives with significant and selective anti-proliferative activities against human cancer cell lines. Notably, 17(*E*)-picolinylidene androstane derivatives were shown to have significant and selective cytotoxic activity against PC3 prostate cancer cells. Preliminary in silico virtual screening and in vitro cytotoxicity studies suggest that A-modified 17(*E*)-picolinylidene androstane derivatives represent promising candidates for the development of a new series of steroid-based compounds for the treatment of prostate cancer, indicating the need for more detailed future studies. The results obtained in the present study could be used to guide the development of a novel series of 17-picolinylidene androstanes (Fig. 7) to

investigate the in vitro kinetics and mechanism of 17α-hydroxylase/17,20 lyase enzymatic inhibition, and/or to conduct more extensive anti-cancer studies using in vivo prostate tumor models.

4. Materials and methods

4.1. Chemical synthesis

4.1.1. General

Melting points were determined using an electrothermal 9100 apparatus and are reported uncorrected. IR spectra were measured on a NEXUS 670 SP-IR spectrometer (wave numbers in cm^{-1}). NMR spectra were recorded on a Bruker AC 250E spectrometer operating at 250 MHz (^1H) and 62.5 MHz (^{13}C), and are reported in ppm (δ-scale) downfield from the tetramethylsilane internal standard; coupling constants (J) are given in Hz. High resolution mass spectra (TOF) were recorded on a 6210 Time-of-Flight LC/MS Agilent Technologies (ESI+) instrument. Chromatographic separations were performed on silica gel columns (Kieselgel 60, 0.063–0.20 mm, Merck). All reagents used were of analytical grade. All solutions were dried over anhydrous sodium sulfate

4.1.2. General procedure for microwave-assisted synthesis of compounds 3 and 4

Compound **1** (0.105 g, 0.278 mmol) or **2** (0.153 g, 0.423 mmol), hydrazine hydrate (0.05 ml, 1.03 mmol for **1** or 0.08 ml, 1.65 mmol for **2**) and ethylene–glycol (1.4 or 2.1 ml, with a catalytic amount of anhydrous Na_2SO_4 (10^{-3} mmol)) were mixed and exposed to microwave irradiation at 195 °C (170 W) for 4 min (for **1**) or at 195 °C (170 W) for 2 min (for **2**). After cooling, the reaction mixture was poured into water (30 ml), and extracted with ethyl acetate (5 × 10 ml). The combined organic extracts were dried and evaporated. The crude product was purified by column chromatography (6 g silica gel, hexane/ethyl acetate 1:2 for **3**, or 10 g, hexane/ethyl acetate 2:1 and 1:1 for **4**) affording pure compound **3** (0.109 g, 100%, mp >260 °C) or pure compound **4** (0.055 g, 35%, mp 257–259 °C), both in the form of a yellow solid.

*17β-Hydroxy-17α-picolyl-androst-4-en-3-on hydrazone (**3**):* IR (KBr) ν/cm^{-1}: 3334, 2938, 2856, 1671, 1629, 1596, 1473, 1437, 1378, 1330, 1240, 1125, 1023, 873, 755; ^1H NMR (250 MHz, $CDCl_3$, ppm) δ: 1.00 (3H, s, H-18), 1.11 (3H, s, H-19), 2.79 (1H, d, J_{gem} = 14.7 Hz, CH_2Py), 3.06 (1H, d, J_{gem} = 14.7 Hz, CH_2Py), 5.98 (1H, s, H-4), 6.67 (2H, bs, NH_2), 7.16 (2H, m, H-3′ i H-5′, Py), 7.63 (1H, td, $J_{4',3'} = J_{4',5'}$ = 7.7 Hz, $J_{4',6'}$ = 1.3 Hz, H-4′, Py), 8.46 (1H, m, H-6′, Py); ^{13}C NMR (62.9 MHz, $CDCl_3$, ppm) δ: 14.14 (C-18), 17.74 (C-19), 21.03, 21.92, 23.89, 32.19, 32.68, 35.46, 35.96, 36.50, 38.30, 39.03, 43.13, 46.38, 50.31, 53.98, 83.37 (C-17), 113.81 (C-4), 121.34 (C-5′, Py), 124.73 (C-3′, Py), 136.76 (C-4′, Py), 147.99 (C-6′, Py), 158.31 (C-3), 160.79 (C-2′, Py), 161.40 (C-5). MS (ESI), m/z: 380.25 (100), 252.51 (28), 223.66 (14).

*17(E)-Picolinylidene-androst-4-en-3-on hydrazone (**4**):* IR (KBr) / cm^{-1}: 2940, 2852, 1653, 1625, 1585, 1560, 1470, 1428, 1373, 1259, 1237, 1215, 1150, 1103, 885, 754; ^1H NMR (250 MHz, $CDCl_3$, ppm) δ: 0.93 (6H, 2s, H-18 and H-19), 5.99 (1H, s, H-4), 6.22 (2H, s, NH_2), 6.45 (1H, s, H-20), 7.04 (1H, m, H-5′, Py), 7.28 (1H, m, H-3′, Py), 7.61 (1H, td, $J_{4',3'} = J_{4',5'}$ = 7.7 Hz, $J_{4',6'}$ = 1.8 Hz, H-4′, Py), 8.56 (1H, d, $J_{6',5'}$ = 4.8 Hz, H-6′, Py); ^{13}C NMR (62.9 MHz, $CDCl_3$, ppm) δ: 17.93 (C-18), 18.79 (C-19), 21.36, 21.89, 24.95, 27.96, 29.78, 32.27, 35.40, 35.56, 38.27, 38.99, 45.76, 53.25, 54.01, 113.93 (C-4), 118.01 (C-20), 120.17 (C-5′, Py), 122.76 (C-3′, Py), 135.77 (C-4′, Py), 149.14 (C-6′, Py), 157.55 (C-17), 158.73 (C-3), 160.16 (C-2′, Py), 161.57 (C-5). MS (ESI), m/z: 376.25 (6, $(M+H)^+$), 360.25 (28), 251.17 (25), 240.51 (100).

*Wolff–Kishner reduction of compound **2**.* Compound **2** (0.204 g, 0.565 mmol), hydrazine hydrate (0.11 ml, 2.27 mmol) and ethylene–glycol (2.8 ml, with a catalytic amount of anhydrous Na_2SO_4 (10–3 mmol)) were mixed and exposed to microwave irradiation at 195 °C (170 W) for 2 min. Then, powdered potassium hydroxide (0.48 g, 8.57 mmol) was added, and the reaction mixture was microwave irradiated at 195 °C (170 W) for 40 min. After cooling, the reaction mixture was poured into water (40 ml), and extracted with ethyl acetate (5 × 10 ml). The combined organic extract was dried and evaporated, to yield crude product which was purified by column chromatography (8 g, hexane/ethyl acetate 5:1) to afford a mixture of compounds **5** and **6** (0.147 g, 75%), in the form of a colorless oil.

*Clemmensen reduction of compound **2**.* Compound **2** (0.208 g, 0.575 mmol) was dissolved in boiling glacial acetic acid (12 ml) to which zinc powder (0.966 g, 14.7 mmol) was added. The reaction mixture was stirred under reflux for 2 h. After cooling, the reaction mixture was filtered (to remove unreacted zinc and zinc acetate), poured into water (30 ml), adjusted to pH 6–7 with saturated $NaHCO_3$, and extracted with dichloromethane (5 × 10 ml). The combined organic layers were dried and concentrated in vacuo to afford crude product. After purification by column chromatography (15 g silica gel, toluene/ethyl acetate 12:1), a mixture of compounds **5** and **6** (0.094 g, 47%) were obtained in the form of a colorless oil.

4.1.3. Mixture of 17(*E*)-picolinyliden-5α-androst-3-ene (5) and 17(*E*)-picolinyliden-5β-androst-3-ene (6)

IR (film) /cm^{-1}: 2935, 1673, 1585, 1469, 1434, 1374, 1233, 1149, 754; ^1H NMR (250 MHz, $CDCl_3$, ppm) δ: 0.89 (3H, s, H-18), 0.99 (3H, s, H-19), 5.31 (2H, m, H-3 from 5α and 5β isomer), 5.56 (1H, dd, J_1 = 9.8 Hz, J_2 = 3.3 Hz, H-4 from 5α isomer), 5.66 (1H, dd, J_1 = 9.9 Hz, J_2 = 3.3 Hz, H-4 from 5β isomer); 6.25 (1H, s, H-20), 7.06 (1H, m, H-5′, Py), 7.30 (1H, m, H-3′, Py), 7.63 (1H, t, $J_{4',3'} = J_{4',5'}$ = 7.7 Hz, H-4′, Py), 8.56 (1H, d, $J_{5',6'}$ = 4.5 Hz, H-6′, Py); ^{13}C NMR (62.9 MHz, $CDCl_3$, ppm) δ: 18.79 (C-18); 21.05; 21.48; 22.36; 22.92 (C-19); 23.46; 24.90; 27.42; 29.89; 31.95; 34.04; 35.44; 35.91; 43.49; 46.16; 53.42; 117.28 (C-20 from 5α isomer); 117.41 (C-20 from 5β isomer); 120.18 (C-5′, Py); 122.81 (C-3′, Py); 125.48 (C-3 from 5α isomer); 127.10 (C-3 from 5β isomer); 131.25 (C-4 from 5α isomer); 132.13 (C-4 from 5β isomer); 136.23 (C-4′, Py); 148.59 (C-6′, Py); 157.32 (C-17); 161.67 (C-2′, Py).

4.1.4. General procedure for synthesis of compounds 12 and 13

To the mixture of 4α,5α- and 4β,5β-epoxides **8** and **9** (0.106 g, 0.294 mmol) or **10** and **11** (0.103 g, 0.272 mmol) hydrazine hydrate (0.15 ml, 3.03 mmol for **8** and **9** or 0.20 ml, 4.12 mmol for **10** and **11**) was added and the reaction mixture was stirred at 120 °C for 30 min. After completion of the reaction, the reaction mixture was dissolved in dichloromethane (10 ml), water was added (50 ml) and the mixture was extracted with dichloromethane (3 × 10 ml). The organic layer was dried, filtered and evaporated, and the crude product was purified by column chromatography (1 g silica gel). Elution with petrol–ether/ethyl acetate 5:1 (for **12**) or petrol–ether/ethyl acetate 6:1 (for **13**) afforded pure compound **12** (0.031 g, 30%), or pure compound **13** (0.053 g, 53%), both in the form of a colorless oil.

*17α-Picolyl-androst-3-ene-5ξ,17β-diol (**12**):* IR (film) /cm^{-1}: 3384, 2934, 2869, 1597, 1570, 1474, 1439, 1379, 1252, 1118, 1066, 1010, 980, 755; ^1H NMR (250 MHz, $CDCl_3$, ppm) δ: 0.95 (3H, s, H-18), 1.00 (3H, s, H-19), 1.95 (2H, m, H-2), 2.83 (1H, d, J_{gem} = 14.3 Hz, CH_2Py), 3.17 (1H, d, J_{gem} = 14.3 Hz, CH_2Py), 5.54 (1H, d, $J_{3,4}$ = 9.9 Hz, H-4), 5.84 (1H, m, H-3), 7.23 (2H, m, H-3′ i H-5′, Py), 7.73 (1H, t, $J_{4',3'} = J_{4',5'}$ = 7.7 Hz, H-4′, Py), 8.48 (1H, d, $J_{6',5'}$ = 5.7 Hz, H-6′, Py); ^{13}C NMR (62.9 MHz, $CDCl_3$, ppm) δ: 14.18 (C-18), 16.49 (C-19), 22.29, 22.39, 23.83, 27.82, 28.78, 32.20, 35.08, 35.41, 35.67, 39.15, 42.55, 43.53, 46.66, 50.55, 71.93 (C-5), 83.37

(C-17), 121.68 (C-5′, Py), 125.36 (C-3′, Py), 130.84 (C-3), 133.60 (C-4), 137.77 (C-4′, Py), 146.86 (C-6′, Py), 160.16 (C-2′, Py). HRMS (TOF), *m*/*z*: for $C_{25}H_{36}NO_2$ $[M+H]^+$ calcd 382.27406; found 382.27241.

*17(E)-Picolinylidene-androst-3-en-5ξ-ol (**13**):* IR (film) /cm^{-1}: 3412, 2933, 1653, 1587, 1566, 1468, 1435, 1374, 1010, 913, 755, 665; ^{1}H NMR (250 MHz, $CDCl_3$, ppm) : 0.88 (3H, s, H-18), 1.01 (3H, s, H-19), 2.65–2.88 (2H, m, H-16a i H-16b), 5.51 (1H, d, $J_{3,4}$ = 9.9 Hz, H-4), 5.81 (1H, m, H-3), 6.30 (1H, s, H-20), 7.09 (1H, m, H-5′, Py), 7.33 (1H, d, $J_{3',4'}$ = 7.8 Hz, H-3′, Py), 7.67 (1H, td, $J_{4',3'}$ = -$J_{4',5'}$ = 7.8 Hz, $J_{4',6'}$ = 1.5 Hz, H-4′, Py), 8.55 (1H, d, $J_{6',5'}$ = 4.3 Hz, H-6′, Py); ^{13}C NMR (62.9 MHz, $CDCl_3$, ppm) δ: 16.41 (C-18), 18.70 (C-19), 22.35, 22.58, 24.90, 27.77, 28.75, 29.89, 34.68, 34.97, 35.49, 39.12, 43.60, 46.12, 53.37, 71.87 (C-5), 116.97 (C-20), 120.35 (C-5′, Py), 122.88 (C-3′, Py), 130.83 (C-3), 133.43 (C-4), 136.75 (C-4′, Py), 148.01 (C-6′, Py), 156.84 (C-17), 161.92 (C-2′, Py). HRMS (TOF), *m*/*z*: for $C_{25}H_{34}NO$ $[M+H]^+$ calcd 364.26349; found 364.26402.

4.1.5. Procedure for the preparation of compound 14

The mixture of 4α,5α- and 4β,5β-epoxides **8** and **9** (0.059 g, 0.149 mmol) was dissolved in 50% ethanol (2 ml), and *p*-toluenesulfonyl-hydrazine (0.028 g, 0.148 mmol) was added. The reaction mixture was stirred at room temperature for 1 h, and then at 55 °C for an additional hour. When the reaction was complete, the mixture was poured into water (10 ml), and extracted with dichloromethane (3 × 10 ml). After work-up, crude product was purified by column chromatography (1 g silica gel, petrol–ether/ethyl acetate 4:1) to give pure compound **14** (0.032 g, 56%, mp 141–142 °C) in the form of a white solid.

*17β-Hydroxy-17α-picolyl-4,5-secoandrost-3-yn-5-one (**14**):* IR (KBr) /cm^{-1}: 3307, 2941, 2116, 1700, 1637, 1597, 1439, 1379, 1323, 1217, 1165, 1123, 1033, 1010, 957, 815, 756; ^{1}H NMR (250 MHz, $CDCl_3$, ppm) δ: 1.01 (3H, s, H-18), 1.12 (3H, s, H-19), 1.93 (1H, t, *J* = 2.3 Hz, ≡CH), 2.84 (1H, d, J_{gem} = 14.3 Hz, CH_2Py), 3.20 (1H, d, J_{gem} = 14.3 Hz, CH_2Py), 7.26 (2H, m, H-3′ i H-5′, Py), 7.76 (1H, m, H-4′, Py), 8.49 (1H, d, $J_{6',5'}$ = 4.7 Hz, H-6′, Py); ^{13}C NMR (62.9 MHz, $CDCl_3$, ppm) δ: 13.74, 14.27 (C-18), 20.61 (C-19), 21.24, 23.80, 30.87, 31.69, 33.57, 35.44, 35.61, 38.04, 42.43, 46.70, 47.42, 50.18, 50.80, 68.07 (C-3), 83.16 (C-4), 84.99 (C-17), 121.86 (C-5′, Py), 125.43 (C-3′, Py), 138.08 (C-4′, Py), 146.65 (C-6′, Py), 159.76 (C-2′, Py), 214.46 (C-5). HRMS (TOF), *m*/*z*: for $C_{25}H_{34}NO_2$ $[M+H]^+$ calcd 380.25841; found 380.25687.

4.2. Cell lines and cell culture

Five human tumor cell lines (breast adenocarcinoma ER−, MDA-MB-231; breast adenocarcinoma ER+, MCF-7; prostate cancer, PC3; cervical carcinoma, HeLa; colon adenocarcinoma, HT-29) and one human noncancerous cell line (normal fetal lung fibroblasts MRC-5), were used in the present study. Cells were grown in Dulbecco's modified Eagle's medium (DMEM) with 4.5% of glucose, supplemented with 10% of fetal calf serum (FCS, NIVNS) and antibiotics: 100 IU mL^{-1} of penicillin and 100 μg mL^{-1} of streptomycin (ICN Galenika). Cells were cultured in flasks (Costar, 25 cm^2) at 37 °C in 100% humidity with 5% CO_2. Only viable cells, as determined by trypan blue dye exclusion, were used in subsequent assays.

4.3. Anti-proliferative activity

Compounds were evaluated for antiproliferative activity using the tetrazolium colorimetric MTT assay, after exposure to test compounds, in concentrations ranging from 10^{-8} to 10^{-4} M, for 48 h. The MTT assay is based on cleavage of 3-(4,5-dimethylthiazol-2-yl)-2,5-diphenyl tetrazolium bromide (MTT) to formazan by mitochondrial dehydrogenases in viable cells. Doxorubicin (DOX) is a nonselective antiproliferative agent, which was used as a general cytotoxicity control. Exponentially growing cells were harvested, counted by trypan blue exclusion, and plated onto 96-well microtiter plates (Costar) at an optimal seeding density of 5000 cells per well, to assure a logarithmic growth rate throughout the assay period. Viable cells were plated in a volume of 90 μL per well, and pre-incubated in complete medium at 37 °C for 24 h to ensure cell stabilization prior to the addition of test compounds. Tested compounds, at 10× the required final concentration, in growth medium (10 μL per well) were added to all wells except controls, and microplates were incubated for 24 h. Wells containing cells without tested compounds were used as a control. Three hours before the end of the incubation period, 10 μL of MTT solution was added to each well. MTT was dissolved in the medium at 5 mg mL^{-1} and filter sterilized, to remove a small amount of insoluble residue present in some batches of MTT. Acidifed 2-propanol (100 μL of 0.04 M HCl in 2-propanol) was added to each well, and mixed thoroughly to dissolve the dark blue crystals. After a few minutes incubation at room temperature (to ensure that all crystals were dissolved), plates were read on a spectrophotometric plate reader (Multiscan MCC340, Labsystems) at 540/690 nm. Wells without cells containing complete medium and MTT only were used as a blank. Antiproliferative activity was expressed as IC_{50} (50% inhibitory concentration).

4.4. Data analysis

Two independent experiments were conducted in quadruplicate for each concentration of tested compound. Mean values and standard deviations (SD) were calculated for each concentration. The IC_{50} value is defined as the dose of compound that inhibits cell growth by 50%. The IC_{50} of each tested compound was determined by median effect analysis.

4.5. X-ray data processing and structure solution

Diffraction data for compound **14** were collected using an Oxford Diffraction Gemini S four-circle goniometer equipped with a Sapphire CCD detector. The crystal-to-detector distance was 45.0 mm and graphite monochromated MoKα (λ = 0.71073 Å) radiation was used for the experiments. The data were reduced using the program CrysAlisPRO.[33] A semiempirical absorption–correction based on the intensities of equivalent reflections was applied, and the data were corrected for Lorentz, polarization, and background effects. The structure was solved by direct methods in the program Sir 97[34] and refined by full-matrix least-squares procedures on F^2 using SHELXL-97 programs[35] as implemented in the WinGX program suite.[36] All nonH atoms were refined anisotropically and H atoms were treated by a mixture of independent and constrained refinement. Crystallographic data and structural co-ordinates for compound **14** were deposited in the Cambridge crystallographic data centre (CCDC 948404), and can be obtained free of charge at http://www.ccdc.cam.ac.uk/conts/retrieving.html [or from the Cambridge crystallographic data centre (CCDC), 12 Union Road, Cambridge CB2 1EZ, UK; fax: +44 (0)1223 336033; email: deposit@ccdc.cam.ac.uk].

4.6. Molecular docking

4.6.1. Protein (receptor) structural co-ordinate preparation

Three-dimensional structural co-ordinates for estrogen receptor α (ERα: PDB ID 1A52), androgen receptor (AR: PDB ID 2AMA), Aromatase (CYP19A1: PDB ID 3EQM) and 17,20-lyase/17α-hydroxylase (CYP17A1: PDB ID 3RUK) were obtained from the protein data bank (http://www.rcsb.org). Co-ordinates for ligands and all water molecules were removed using a text editor. Hydrogen atoms and Gasteiger partial charges were added using the script

'receptor.c' in VEGA ZZ 3.0.1.[37] Nonpolar hydrogen atoms were merged in VEGA ZZ and receptor co-ordinate files saved in PDBQT format for docking simulations.

4.6.2. Ligand structural co-ordinate preparation

Based on the X-ray crystal structures of compounds **1**, **2**,[16] and **14**, 3D structural models of compounds **1–14** were created in AVOGADRO 1.0.3 (http://avogadro.openmolecules.net/).[23] Hydrogen atoms were added and ligand geometries were optimized (MMFF94 force field: 500 steps of conjugate gradient energy minimization followed by 500 steps of steepest descent energy minimization with a convergence setting of 10×10^{-7}) in the program AVOGADRO. Nonpolar hydrogen atoms were merged and Gasteiger partial charges partial charges were calculated using the script 'ligand.c' in VEGA ZZ 3.0.1 and the resulting ligand co-ordinate files were saved in PDBQT format.

4.6.3. Grid map calculations

Autodock grid maps were calculated for each receptor using AutoGrid 4,[27] based on the co-ordinates of each protein crystal structure. Individual grid maps were centered on each protein molecule and a maximum grid box size was chosen (covering the entire protein), to enable unbiased docking. A default grid spacing of 0.375 Å was used. Maps were calculated for each atom type in each ligand along with an electrostatic and desolvation map using a dielectric value of −0.1465.

4.6.4. Molecular docking simulations

The initial ligand position, orientation and dihedral offset were set as random. The number of torsional degrees of freedom for each ligand was determined in AutoDockTools.[27] Molecular docking simulations were conducted using the Larmarckian genetic algorithm. The maximum number of energy evaluations was 2,500,000 and the GA population size was 150. A total of 10 hybrid GA-LS runs were performed for each simulation. Results were visualized using the program PyMol (http://www.pymol.org/) and compared with X-ray crystal structures of ligand bound receptor complexes: estrogen receptor α (ERα: PDB ID 1A52), androgen receptor (AR: PDB ID 2AMA), Aromatase (CYP19A1: PDB ID 3EQM) and 17,20-lyase/17α-hydroxylase (CYP17A1: PDB ID 3RUK). N–Fe ligand–receptor bond distances for CYP17A1 bound ligands were measured in PyMol. Autodock and AutoGrid calculations were conducted remotely at the National Biomedical Computational Resource (http://nbcr-222.ucsd.edu/opal2)[25] using the PyRx virtual screening tool.[26] All control docking simulations using ligands present in X-ray crystal structures of the receptors were able to reproduce the ligand–protein interaction geometries present in the respective crystal structures (see Fig. 3). Based on these control docking simulations, predicted binding energies $\leqslant -10.00$ kcal/mol were considered to be indicative of strong binding.

Acknowledgment

We would like to thank the Ministry of Education and Science of the Republic of Serbia for financial support (Grant No. 172021).

Supplementary data

Supplementary data associated with this article can be found, in the online version, at http://dx.doi.org/10.1016/j.bmc.2013.09.063. These data include MOL files and InChiKeys of the most important compounds described in this article.

References and notes

1. Yadav, M. R.; Sabale, P. M.; Giridhar, R.; Zimmer, C.; Hartmann, R. W. *Steroids* **2012**, *77*, 850.
2. Li, X.; Singh, S. M.; Cote, J.; Laplante, S.; Veilleux, R.; Labrie, F. *J. Med. Chem.* **1995**, *38*, 1456.
3. Mitchell, H. J.; Dankulich, W. P.; Hartman, G. D.; Prueksaritanont, T.; Schmidt, A.; Vogel, R. L.; Bai, C.; McElwee-Witmer, S.; Zhang, H. Z.; Chen, F.; Leu, C. T.; Kimmel, D. B.; Ray, W. J.; Nantermet, P.; Gentile, M. A.; Duggan, M. E.; Meissner, R. S. *J. Med. Chem.* **2009**, *52*, 4578.
4. Salvador, J. A.; Pinto, R. M.; Silvestre, S. M. *J. Steroid Biochem. Mol. Biol.* **2013**.
5. He, Q.; Jiang, D. *Leuk. Res.* **1999**, *23*, 369.
6. Minorics, R.; Szekeres, T.; Krupitza, G.; Saiko, P.; Giessrigl, B.; Wolfling, J.; Frank, E.; Zupko, I. *Steroids* **2011**, *76*, 156.
7. Roy, J.; DeRoy, P.; Poirier, D. *J. Comb. Chem.* **2007**, *9*, 347.
8. Latham, K. A.; Zamora, A.; Drought, H.; Subramanian, S.; Matejuk, A.; Offner, H.; Rosloniec, E. F. *J. Immunol.* **2003**, *171*, 5820.
9. Hosking, D.; Chilvers, C. E.; Christiansen, C.; Ravn, P.; Wasnich, R.; Ross, P.; McClung, M.; Balske, A.; Thompson, D.; Daley, M.; Yates, A. J. *N. Eng. J. Med.* **1998**, *338*, 485.
10. Ondre, D.; Wolfling, J.; Toth, I.; Szecsi, M.; Julesz, J.; Schneider, G. *Steroids* **2009**, *74*, 1025.
11. Valachis, A.; Mauri, D.; Polyzos, N. P.; Mavroudis, D.; Georgoulias, V.; Casazza, G. *Crit. Rev. Oncol. Hematol.* **2010**, *73*, 220.
12. McGuire, W. L.; Carbone, P. O.; Vollmer, E. P. *Estrogen Receptors in Human Breast Cancer*; Raven Press: New York, 1975.
13. Handratta, V. D.; Jelovac, D.; Long, B. J.; Kataria, R.; Nnane, I. P.; Njar, V. C.; Brodie, A. M. *J. Steroid Biochem. Mol. Biol.* **2004**, *92*, 155.
14. DeVore, N. M.; Scott, E. E. *Nature* **2012**, *482*, 116.
15. Bruno, R. D.; Gover, T. D.; Burger, A. M.; Brodie, A. M.; Njar, V. C. *Mol. Cancer Ther.* **2008**, *7*, 2828.
16. Djurendic, E.; Daljev, J.; Sakac, M.; Canadi, J.; Santa, S. J.; Andric, S.; Klisuric, O.; Kojic, V.; Bogdanovic, G.; Djurendic-Brenesel, M.; Novakovic, S.; Gasi, K. P. *Steroids* **2008**, *73*, 129.
17. Gasi, K. M.; Brenesel, M.; Djurendic, E. A.; Sakac, M. N.; Canadi, J. J.; Daljev, J. J.; Armbruster, T.; Andric, S.; Sladic, D. M.; Bozic, T. T.; Novakovic, I. T.; Juranic, Z. D. *Steroids* **2007**, *72*, 31.
18. Djurendic, E. A.; Ajdukovic, J. J.; Sakac, M. N.; Csanadi, J. J.; Kojic, V. V.; Bogdanovic, G. M.; Penov Gasi, K. M. *Eur. J. Med. Chem.* **2012**, *54*, 784.
19. Gupta, A.; Sathish Kumar, B.; Negi, A. S. *J. Steroid Biochem. Mol. Biol.* **2013**.
20. Gasi, K. M.; Gakovic, A. R.; Ajdukovic, J. J.; Djurendic-Brenesel, M. D.; Djurendic, E. A.; Savic, M. P.; Sakac, M. N. *Acta Period. Technol.* **2010**, *41*, 169.
21. Kirk, D. N.; Hartshorn, M. P. *Steroid Reaction Mechanisms*; Elsevier Publishing: Amsterdam, 1968.
22. Stewart, J. J. *J. Mol. Model.* **2007**, *13*, 1173.
23. Hanwell, M. D.; Curtis, D. E.; Lonie, D. C.; Vandermeersch, T.; Zurek, E.; Hutchison, G. R. *J. Cheminform.* **2012**, *4*, 17.
24. David-Beabes, G. L.; Overman, M. J.; Petrofski, J. A.; Campbell, P. A.; de Marzo, A. M.; Nelson, W. G. *Int. J. Oncol.* **2000**, *17*, 1077.
25. Ren, J.; Williams, N.; Clementi, L.; Krishnan, S.; Li, W. W. *Nucleic Acids Res.* **2010**, *38*, W724.
26. Wolf, L. K. *Chem. Eng. News* **2009**, *87*, 31.
27. Morris, G. M.; Huey, R.; Lindstrom, W.; Sanner, M. F.; Belew, R. K.; Goodsell, D. S.; Olson, A. J. *J. Comput. Chem.* **2009**, *30*, 2785.
28. Ghosh, D.; Griswold, J.; Erman, M.; Pangborn, W. *Nature* **2009**, *457*, 219.
29. Tanenbaum, D. M.; Wang, Y.; Williams, S. P.; Sigler, P. B. *Proc. Natl. Acad. Sci. U.S.A.* **1998**, *95*, 5998.
30. Pereira de Jesus-Tran, K.; Cote, P. L.; Cantin, L.; Blanchet, J.; Labrie, F.; Breton, R. *Protein Sci.* **2006**, *15*, 987.
31. Handratta, V. D.; Vasaitis, T. S.; Njar, V. C. *J. Med. Chem.* **2005**, *48*, 2972.
32. Tetko, I. V.; Gasteiger, J.; Todeschini, R.; Mauri, A.; Livingstone, D.; Ertl, P.; Palyulin, V. A.; Radchenko, E. V.; Zefirov, N. S.; Makarenko, A. S.; Tanchuk, V. Y.; Prokopenko, V. V. *J. Comput. Aided Mol. Des.* **2005**, *19*, 453.
33. Agilent. Agilent Technologies: Yarnton, Oxfordshire, CrysAlis PRO, England, 2010.
34. Altomare, A.; Burla, M. C.; Cavalli, M.; Cascarano, G.; Giacovazzo, C.; Gagliardi, A.; Moliterni, A. G.; Polidori, G.; Spagna, R. J. *Appl. Crystallogr.* **1999**, *32*, 115.
35. Sheldrick, G. M. *Acta Crystallogr.* **2008**, *A64*, 112.
36. Farrugia, L. J. J. *Appl. Crystallogr.* **1999**, *32*, 837.
37. Pedretti, A.; Villa, L.; Vistoli, G. *J. Comput. Aided Mol. Des.* **2004**, *18*, 167.